Stabilized jellium: Structureless pseudopotential model for the cohesive and surface properties of metals

John P. Perdew, Huy Q. Tran, and Elizabeth D. Smith
Department of Physics and Quantum Theory Group, Tulane University, New Orleans, Louisiana 70118
(Received 22 June 1990)

The ions in a simple metal act on the valence electrons via a pseudopotential. The long-range part is represented by the electrostatic potential from the positive background of the jellium model. The short-range part can be simulated by a constant (over the interior of the metal), chosen to stabilize the metal at its observed bulk valence-electron density. In this structureless pseudopotential model, the bulk properties of a metal depend only upon valence z and bulk density parameter r_s, while the surface properties depend upon r_s alone (an experimental trend heretofore not understood). These properties are calculated in closed analytic form, and the anomalies of the jellium model (negative surface energy for $r_s \approx 2$; negative bulk modulus for $r_s \approx 6$) are found to be rectified. The new model, perhaps the simplest one viable for all r_s, may also be used to study interfaces, metallic clusters, vacancies, electromagnetic response, etc. A variant of the model, which simulates the effects of atomic corrugation, predicts the crystal face dependence of surface properties. This dependence is strong for the electron-density profile, but not for the surface energy, work function, and distance from the centroid of excess charge to the first lattice plane. Results are presented for metallic hydrogen as well as for Al, Pb, Zn, Mg, Ca, Li, Sr, Ba, Na, K, Rb, and Cs.

I. INTRODUCTION

Because simple *sp*-bonded metals are nearly-free-electron systems, they are often described theoretically by the jellium model.[1-3] In jellium, the ions are smeared into a positive background,

$$n_+(\mathbf{r}) = \bar{n}\Theta(\mathbf{r}) , \tag{1}$$

where

$$\bar{n} = 3/4\pi r_s^3 = k_F^3/3\pi^2 \tag{2}$$

is the average valence-electron density. Here, $\Theta(\mathbf{r})$ equals 1 inside a surface of zero thickness, and 0 outside. The valence electrons, with density $n(\mathbf{r})$, neutralize this background, except in a region of atomic thickness around the surface. For $r_s \approx 4$ bohr, where bulk jellium is stable, the jellium model provides a useful description of the cohesive and surface properties of the simple metals, but anomalies arise for densities where bulk jellium is far out of equilibrium: (1) For $r_s \approx 2$, the jellium surface energy is negative;[1] (2) For $r_s \approx 6$, the jellium bulk modulus is negative.[4]

These deficiencies of the jellium model are rectified by pseudopotential corrections.[1-5] The Ashcroft empty-core pseudopotential[5] for the interaction between an ion of charge z and an electron at r is

$$w(r) = \begin{cases} -z/r & (r > r_c) \\ 0 & (r < r_c), \end{cases} \tag{3}$$

where the core radius r_c is usually fitted to some measured property. (All equations are expressed in atomic units. The unit of distance is 1 bohr $= 0.5292 \times 10^{-8}$ cm, and the unit of energy is 1 hartree $= 27.21$ eV $= 4.360 \times 10^{-11}$ erg.) The "difference potential" $\delta v(\mathbf{r})$ (between the pseudopotential of a lattice of ions and the electrostatic potential of the jellium positive background) may be treated perturbatively,[1-6] variationally,[7-10] or exactly. However, the simplicity and universality of the jellium model are lost: the cohesive and surface properties now depend upon valence z and crystal structure, as well as upon r_s.

In Sec. II, we present a "structureless pseudopotential model," which may be the simplest viable picture for metals at all r_s. The actual difference potential $\delta v(\mathbf{r})$ is replaced by one which is constant in the bulk of the metal, and zero outside. This constant, the average of $\delta v(\mathbf{r})$ over a Wigner-Seitz spherical cell, is chosen to make the metal stable at its observed valence-electron density (i.e., the calculated pressure P vanishes at the observed r_s). While the Ashcroft pseudopotential is very "hard" or structured, the structureless pseudopotential is the "softest" one that can be imagined. In this model, the predicted bulk properties of a metal [binding energy per electron $-\varepsilon$, bulk modulus B, and zero-temperature equation of state $P(r_s)$] depend only upon z and r_s (Sec. III), while flat-surface properties (surface energy σ and work function W) depend upon r_s *alone* (Sec. IV). This simple model may prove useful, not just for the properties considered here but wherever the jellium model is commonly used, e.g., in the theory of metallic clusters,[3,11] vacancies, interfaces, electromagnetic response, etc.

A variant of the model (Sec. V), which takes account of surface corrugation on the atomic scale, predicts the crystal face dependence of surface properties such as the surface energy σ, work function W, planar-averaged electron density profile $n(x)$, and centroid of excess charge x_0. We apply the model to twelve simple metals con-

sidered in earlier work,[7-9] plus metastable metallic hydrogen.[12] (A nonmonatomic form of metallic hydrogen may have been created recently by the intense pressure of a diamond anvil.[13])

The structureless pseudopotential model evolves from previous work, most directly from the "variational self-consistent method" of Monnier and Perdew,[7] and the "pseudojellium model" of Utreras-Díaz and Shore.[11,14] The most important new features in the present work are the requirement of bulk mechanical stability and the complete neglect of crystal structure. These same approximations were developed independently by Rose and Shore[15] and by us.[16] The importance of bulk stability for the calculation of bulk and surface properties is well known. Ashcroft and Langreth[4] imposed this condition to determine the zeroth Fourier coefficient of the pseudopotential in their calculation of bulk moduli. In the words of Allen and Rice,[17] "the pressing need for a pseudopotential or other correction to the jellium model . . . is more a reflection of bulk instability than of differences attributable solely to the discrete nature of the ions."

That is the essential physical picture behind our work. But in order to reduce the cohesive and surface properties to closed analytic form, we make some nonessential additional approximations. (a) Complete neglect of crystal structure, via use of the Wigner-Seitz spherical cell and neglect of the band-structure energy (Sec. II). (b) Use of the fourth-order density-gradient expansion for the electron kinetic energy, and the local-density approximation for exchange and correlation (Sec. II). Under approximation (a), this second approximation introduces no additional error into the bulk properties calculated in Sec. III. (c) A simple variational form for the electron density profile near a flat surface (Sec. IV), similar to the one used in Perdew's "simple analytic model"[18] for the jellium surface. (d) A one-dimensional simulation of the three-dimensional problem posed by the atomic corrugation of the surface (Sec. V). This simulation resembles the "variational self-consistent method" of Monnier and Perdew,[7] but incorporates a new perspective on the face dependence of the surface energy.[19]

With these approximations, the cohesive and surface properties are calculated here in closed analytic form, from which it is easy to see what is important and to what degree. That is not always possible in more detailed calculations for individual metals.

II. SIMPLIFIED ENERGY FUNCTIONAL

The total energy for a system of valence electrons and ions is given by Eq. (2.1) of Monnier and Perdew.[7] The average energy per valence electron in the bulk is

$$\varepsilon = t_s(\bar{n}) + \varepsilon_{xc}(\bar{n}) + \bar{w}_R + \varepsilon_M + \varepsilon_{bs} , \tag{4}$$

where $t_s(\bar{n})$ and $\varepsilon_{xc}(\bar{n})$ are the kinetic and exchange-correlation contributions for a uniform electron gas of density $\bar{n}$:

$$t_s(\bar{n}) = 3k_F^2/10 , \tag{5}$$

$$\varepsilon_{xc}(\bar{n}) = -3k_F/4\pi + \varepsilon_c(\bar{n}) . \tag{6}$$

$\bar{w}_R$ is the average value of the repulsive or non-Coulombic part of the pseudopotential and ε_M is the average Madelung or electrostatic energy of a collection of point ions embedded in a uniform negative background of density $\bar{n}$. All nonuniformity of the true electron density $n(\mathbf{r})$ is contained in the band-structure energy ε_{bs}. For the Ashcroft pseudopotential of Eq. (3),

$$\bar{w}_R = \frac{1}{z}\int_0^{r_c} dr\, 4\pi r^2 \bar{n}\frac{z}{r} = 2\pi\bar{n}r_c^2 . \tag{7}$$

Assuming a monatomic, nearly-close-packed Bravais lattice of ions (face-centered-cubic, body-centered-cubic, or hexagonal-close-packed with near-ideal $c/a \approx 1.633$), the Wigner-Seitz polyhedral unit cell may be replaced by a sphere of radius

$$r_0 = z^{1/3} r_s . \tag{8}$$

The Madelung energy then arises from the interaction between a uniform negative background inside the Wigner-Seitz sphere and a point ion of charge z at its center:

$$\frac{1}{z}\int_0^{r_0} dr\, 4\pi r^2 \bar{n}\left[\frac{-z}{r}\right] = -3z/2r_0 \tag{9}$$

plus the electrostatic self-energy of the uniform negative background inside the sphere:

$$\bar{\varepsilon} = \frac{1}{2z}\int_0^{r_0} dr\, 4\pi r^2 \bar{n} V(r) = 3z/5r_0 , \tag{10}$$

where

$$V(r) = \begin{cases} \dfrac{z}{r_0}\left[\dfrac{3}{2} - \dfrac{r^2}{2r_0^2}\right] & (r < r_0) \\ z/r \quad (r > r_0). \end{cases} \tag{11}$$

Thus

$$\varepsilon_M = -9z/10r_0 . \tag{12}$$

Now consider a finite crystal, with a surface. Imagine a fictitious positive background $n_+(\mathbf{r})$ of the form of Eq. (1), with the sharp surface of $\Theta(\mathbf{r})$ cut along the exposed boundaries of the polyhedral (or spherical) Wigner-Seitz cells. The jellium-model total energy, as a functional of the electron density $n(\mathbf{r})$, is

$$E_{jell}[n,n_+] = T_s[n] + E_{xc}[n] + \tfrac{1}{2}\int d^3r\, \phi([n,n_+];\mathbf{r})[n(\mathbf{r}) - n_+(\mathbf{r})] , \tag{13}$$

where

$$\phi([n,n_+];\mathbf{r}) = \int d^3r'[n(\mathbf{r}') - n_+(\mathbf{r}')]/|\mathbf{r}' - \mathbf{r}| \tag{14}$$

is the jellium electrostatic potential. $E_{xc}[n]$ is the exchange-correlation energy, which we represent in the

local-density approximation[20] as

$$E_{xc}[n]=\int d^3r n(\mathbf{r})\varepsilon_{xc}(n(\mathbf{r}))\ , \tag{15}$$

using the accurate electron-gas correlation energy $\varepsilon_c(n)$ of Vosko, Wilk, and Nusair.[21] (Essentially the same results are obtained from the parametrization of Perdew and Zunger.[22]) $T_s[n]$ is the noninteracting kinetic energy, which could be evaluated exactly by the Kohn-Sham orbital method.[20] Instead, we use the fourth-order density-gradient expansion:[23]

$$T_s[n]=\int d^3r n t_s(n)+\tfrac{1}{72}\int d^3r\frac{|\nabla n|^2}{n}+\frac{(3\pi^2)^{-2/3}}{540}\int d^3r n^{1/3}\left[\left[\frac{\nabla^2 n}{n}\right]^2-\frac{9}{8}\left[\frac{\nabla^2 n}{n}\right]\left|\frac{\nabla n}{n}\right|^2+\frac{1}{3}\left|\frac{\nabla n}{n}\right|^4\right]. \tag{16}$$

Two corrections are needed to transform this jellium into a real metal. The first subtracts from the jellium energy functional the spurious electrostatic self-repulsion energy of the positive background in each cell, i.e., it adds

$$-\bar{\varepsilon}\int d^3r n_+(\mathbf{r}) \tag{17}$$

to Eq. (13), as in the work of Utreras-Díaz and Shore.[14] (The electrostatic repulsion between positive charges in different cells is described adequately by this jellium model.) The second correction adds the interaction between the electrons and the "difference potential" $\delta v(\mathbf{r})$ described in the Introduction,

$$\int d^3r\delta v(\mathbf{r})n(\mathbf{r})\ . \tag{18}$$

We model $\delta v(r)$ to have the following properties. (i) It tends to a constant deep inside the metal. (ii) It yields the correct bulk energy ε [Eq. (4)] and bulk chemical potential

$$\mu_{bulk}=\mu_s(\bar{n})+\mu_{xc}(\bar{n})+\langle\delta v\rangle_{WS}+\mu_{bs}\ . \tag{19}$$

Here,

$$\mu_{xc}(n)=\frac{d}{dn}[n\varepsilon_{xc}(n)] \tag{20}$$

and

$$\langle\delta v\rangle_{WS}=\frac{1}{z}\int_0^{r_0}dr\,4\pi r^2\bar{n}[w(r)+V(r)]$$
$$=\bar{\varepsilon}+\varepsilon_M+\bar{w}_R \tag{21}$$

is the average of $\delta v(\mathbf{r})$ over the volume of the Wigner-Seitz spherical cell. The result of this average contains $\bar{\varepsilon}$, which is needed to cancel the $-\bar{\varepsilon}$ of Eq. (17) in the bulk of the metal.

The band-structure energies ε_{bs} and μ_{bs} were estimated for a number of simple metals by Monnier and Perdew.[7] They typically fall in the range between 0 and -0.5 eV, and will be neglected in our simplified model [a choice that is consistent with property (i) above]. With this approximation, the simplest model for $\delta v(\mathbf{r})$ is

$$\langle\delta v\rangle_{WS}\Theta(\mathbf{r})\ . \tag{22}$$

Since $n_+(\mathbf{r})$ satisfies Eq. (1), and $\Theta^2(\mathbf{r})=\Theta(\mathbf{r})$, the simplified energy function from Eqs. (13), (17), (18), and (22) may be rearranged as

$$E_{pseudo}[n,n_+]=E_{jell}[n,n_+]+(\varepsilon_M+\bar{w}_R)\int d^3r n_+(\mathbf{r})$$
$$+\langle\delta v\rangle_{WS}\int d^3r\Theta(\mathbf{r})[n(\mathbf{r})-n_+(\mathbf{r})]\ . \tag{23}$$

The effective one-electron potential of the Kohn-Sham orbital theory becomes

$$\frac{\delta}{\delta n(\mathbf{r})}(E_{pseudo}[n,n_+]-T_s[n])$$
$$=\phi([n,n_+];\mathbf{r})+\mu_{xc}(n(\mathbf{r}))+\langle\delta v\rangle_{WS}\Theta(\mathbf{r})\ . \tag{24}$$

It remains to determine the Ashcroft core radius r_c of Eq. (7) from the bulk stability condition. When $\bar{n}$ is the equilibrium density,

$$\frac{d}{d\bar{n}}[t_s(\bar{n})+\varepsilon_{xc}(\bar{n})+\varepsilon_M+\bar{w}_R]=0\ . \tag{25}$$

Solving Eq. (25), we find

$$r_c=\left[-\frac{2}{15}\left[\frac{9\pi}{4}\right]^{2/3}r_s+\frac{1}{6\pi}\left[\frac{9\pi}{4}\right]^{1/3}r_s^2\right.$$
$$\left.+\tfrac{1}{5}z^{2/3}r_s^2+\tfrac{2}{9}r_s^4\frac{d\varepsilon_c}{dr}\right]^{1/2}, \tag{26}$$

where r_s is the equilibrium density parameter. Since

$$\langle\delta v\rangle_{WS}=\bar{n}\frac{d}{d\bar{n}}(\varepsilon_M+\bar{w}_R) \tag{27}$$

at any density, we find at the equilibrium density

$$\langle\delta v\rangle_{WS}=-\bar{n}\frac{d}{d\bar{n}}[t_s(\bar{n})+\varepsilon_{xc}(\bar{n})]$$
$$=-\frac{1}{5}\left[\frac{9\pi}{4}\right]^{2/3}r_s^{-2}$$
$$+\frac{1}{4\pi}\left[\frac{9\pi}{4}\right]^{1/3}r_s^{-1}+\tfrac{1}{3}r_s\frac{d\varepsilon_c}{dr_s}\ . \tag{28}$$

While the second term on the right-hand side of Eq. (23) is a correction to the jellium bulk energy depending upon both z and r_s, the third term is a correction to the jellium surface energy depending upon r_s alone. The total energy of the stabilized-jellium described by Eqs. (23)–(28) is the work needed to assemble the crystal, starting from isolated electrons and stabilized-jellium ions. A stabilized-

jellium ion is a sphere of radius r_0 containing positive charge of uniform density $\bar{n}$ (the equilibrium bulk density). This ion interacts with an electron via the soft pseudopotential

$$w'(r)=\begin{cases}-z/r & (r>r_0)\\ -V(r)+\langle \delta v\rangle_{\rm WS} & (r<r_0).\end{cases} \tag{29}$$

The energy functional (23) is constructed under the explicit assumption [see Eq. (10)] that each Wigner-Seitz cell approximates a sharp-boundaried sphere. This functional should *not* be used for a positive background with a diffuse surface. If so misapplied, it will predict a large relaxation of the positive charge at the surface, with a substantial resultant lowering of the surface energy. Such predictions contradict theory and experiment for lattice relaxation at a crystalline surface.[24]

The band-structure energies neglected in this section might be incorporated via the pseudojellium model of Utreras-Díaz and Shore,[14] or by the following generalization of Eq. (23):

$$E_{\rm pseudo}[n,n_+]=E_{\rm jell}[n,n_+]+\int d^3r\left[-\frac{9}{10}z^{2/3}\left[\frac{4\pi n_+}{3}\right]^{1/3}+2\pi r_c^2 n_+ +\varepsilon_{\rm bs}(n_+)\right]n_+ +\int d^3r\left[-\frac{3}{10}z^{2/3}\left[\frac{4\pi n_+}{3}\right]^{1/3}+2\pi r_c^2 n_+ +\mu_{\rm bs}(n_+)\right](n-n_+)\,, \tag{30}$$

which satisfies properties (i) and (ii) above.

III. BULK COHESIVE PROPERTIES

As a first test of the structureless pseudopotential model, we consider the bulk cohesive properties. The Ashcroft core radius r_c is a constant for each metal determined from the valence and observed equilibrium density, via Eq. (26). Table I displays the values so determined, which turn out to be similar to the standard values[4,5] for the simple metals other than Pb.

The energy per electron for the metal at *any* r_s is

$$\varepsilon=\frac{3}{10}\left[\frac{9\pi}{4}\right]^{2/3}\frac{1}{r_s^2}-\frac{3}{4\pi}\left[\frac{9\pi}{4}\right]^{1/3}\frac{1}{r_s} +\varepsilon_c(\bar{n})+\frac{3}{2}\frac{r_c^2}{r_s^3}-\frac{9}{10}\frac{z^{2/3}}{r_s}\,. \tag{31}$$

The last two terms in Eq. (31) are absent in the jellium

TABLE I. Bulk cohesive properties of simple metals. The valence z and equilibrium density parameter r_s determine the Ashcroft core radius r_c. The binding energy per valence electron, $-\varepsilon$, and the bulk modulus B are compared for the jellium model, the structureless pseudopotential model, and experiment. The "experimental" values for H are actually theoretical values from Ref. 12. Values in parentheses are computed with an effective valence $z^*=1$.

	z	r_s (bohr)	r_c (bohr)	$-\varepsilon$ (eV) jell	$-\varepsilon$ (eV) pseudo	$-\varepsilon$ (eV) expt.	B (Mbar) jell	B (Mbar) pseudo	B (Mbar) expt.
H	1	1.58	0.00	−2.80	12.70	14.20	6.326	1.802	1.51
Al	3	2.07	1.11	0.21	19.10	18.88	1.432	1.577	0.722
	(1)		(0.56)		(10.58)	(9.38)		(0.750)	
Pb	4	2.30	1.46	0.88	20.57	24.68	0.788	1.288	0.430
	(1)		(0.72)		(9.78)	(9.45)		(0.525)	
Zn	2	2.30	1.07	0.88	13.95	14.35	0.788	0.819	0.598
	(1)		(0.72)		(9.78)	(10.74)		(0.525)	
Mg	2	2.65	1.31	1.49	12.38	12.10	0.344	0.487	0.354
	(1)		(0.95)		(8.76)	(9.16)		(0.320)	
Ca	2	3.27	1.74	1.96	10.33	9.91	0.092	0.222	0.152
	(1)		(1.33)		(7.40)	(7.95)		(0.150)	
Li	1	3.28	1.33	1.97	7.38	7.02	0.091	0.149	0.116
Sr	2	3.57	1.94	2.05	9.56	9.22	0.051	0.160	0.116
	(1)		(1.51)		(6.87)	(7.42)		(0.109)	
Ba	2	3.71	2.04	2.08	9.24	8.56	0.038	0.138	0.103
	(1)		(1.59)		(6.66)	(7.11)		(0.095)	
Na	1	3.99	1.76	2.10	6.26	6.25	0.022	0.072	0.068
K	1	4.96	2.33	2.06	5.19	5.28	0.002	0.032	0.032
Rb	1	5.23	2.49	2.03	4.95	5.03	0.000	0.026	0.031
Cs	1	5.63	2.72	1.98	4.64	4.70	−0.001	0.020	0.020

model. The binding energy per electron, $-\varepsilon$, is compared in Table I with

$$\frac{1}{z}\left[\sum_{i=1}^{z} I_i + \varepsilon_{\rm coh}\right], \tag{32}$$

where I_i is the measured ith ionization energy[25] of the separated atom, and $\varepsilon_{\rm coh}$ is the cohesive energy.[26] While the jellium model fails for all the metals, the structureless pseudopotential model is satisfactory, again with the exception of Pb.

The pressure for a metal of energy E, volume V, and electron number N is

$$P=-\left[\frac{\partial E}{\partial V}\right]_N=\frac{-1}{4\pi r_s^2}\frac{\partial \varepsilon}{\partial r_s}, \tag{33}$$

where all derivatives are taken at constant r_c. Figure 1 shows the equation of state (P versus r_s) for monatomic metallic hydrogen ($z=1, r_c=0$), which is stable at $r_s \approx 1.6$. The structureless pseudopotential model predicts an equation of state very similar to the third-order calculation of Ashcroft and Hammerberg.[12] On the other hand, jellium can only be held at such a high energy by several Mbars of external pressure.

The bulk modulus or inverse compressibility is

$$B=-V\left[\frac{\partial P}{\partial V}\right]_N=\frac{1}{12\pi}\left[\frac{1}{r_s}\frac{\partial^2 \varepsilon}{\partial r_s^2}-\frac{2}{r_s^2}\frac{\partial \varepsilon}{\partial r_s}\right]. \tag{34}$$

As shown in Table I, the jellium bulk modulus is actually negative at the density of Cs ($r_s=5.63$), but the structureless pseudopotential model predicts a positive bulk modulus for all the metals. Reasonable agreement with experiment[26] is obtained for the monovalent metals, but not for the polyvalents, where band-structure effects make an important contribution to the bulk modulus.[4] This problem can be evaded by using an effective valence $z^*=1$ for all the metals (Table I), i.e., by replacing each Wigner-Seitz cell by z cells, each of volume $4\pi r_s^3/3$. With this choice (which we recommend), *all* the properties of metals become functions of r_s alone, as in the jellium model.

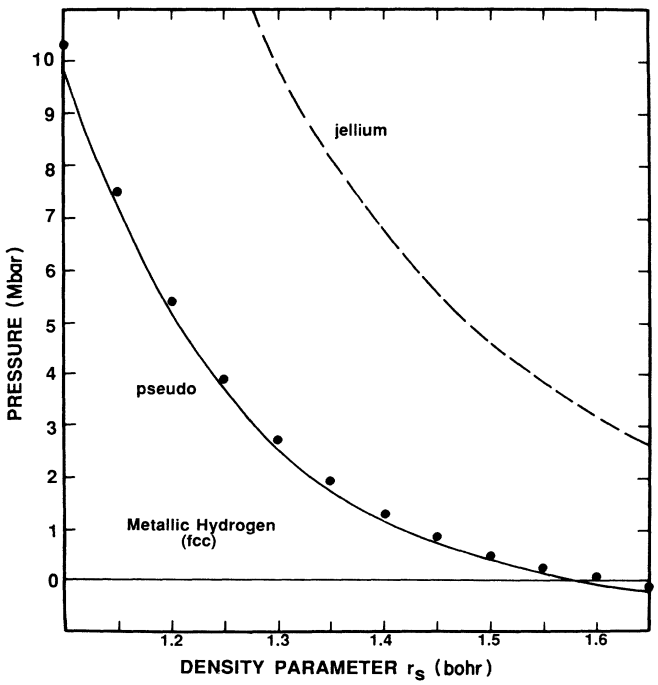

FIG. 1. Equation of state for jellium compared to that for monatomic metallic hydrogen, as calculated in the structureless pseudopotential model (solid curve) and in the third-order expansion of Ref. 12 (dots). (1 hartree/bohr^3=294.2 Mbar).

IV. FLAT-SURFACE PROPERTIES

Consider a flat or planar surface, for which $\Theta(\mathbf{r})$ of Eq. (1) equals $\Theta(-x)$, a step function that vanishes for $x>0$. The electron density $n(x)$ then varies only in the x direction. The surface energy (energy needed to create a unit area of new surface) is found from Eq. (23):

$$\sigma_{\rm pseudo}[n,n_+]=\sigma_{\rm jell}[n,n_+]+\langle \delta v\rangle_{\rm WS}\int_{-\infty}^{0} dx[n(x)-\bar{n}], \tag{35}$$

where $\sigma_{\rm jell}[n,n_+]$ is the standard jellium surface-energy functional, containing kinetic, exchange-correlation, and electrostatic terms.[1] Since the bulk electron density is fixed at $\bar{n}$, the electron density profile $n(x)$ should minimize Eq. (35), subject to the constraint

$$\int_{-\infty}^{\infty} dx[n(x)-\bar{n}\Theta(-x)]=0. \tag{36}$$

The work function (minimum energy needed to remove one electron from the metal) may be evaluated from the displaced-profile change-in-self-consistent-field (DPΔSCF) expression[8,27]

$$W[n,n_+]=\phi([n,n_+];\infty)-\phi([n,n_+];0)-[t_s(\bar{n})+\varepsilon_{\rm xc}(\bar{n})]+\langle \delta v\rangle_{\rm WS}\int_{-\infty}^{0} dx\frac{1}{\bar{n}}\frac{dn(x)}{dx}, \tag{37}$$

which is more accurate than the standard Koopmans expression when $n(x)$ is found by variation of a finite number of parameters.

Following Perdew's "simple analytic model"[18] for the jellium surface, we write

$$n(x)=\bar{n}f(\gamma k_s x), \tag{38}$$

where

$$k_s=\left[\frac{4k_F}{\pi}\right]^{1/2} \tag{39}$$

is the bulk Thomas-Fermi screening wave vector and γ is a scale parameter chosen to minimize Eq. (35); larger γ means a narrower surface region. For convenience, we modify the shape function:

$$f(y)=\begin{cases}1+b_0e^{y}+b_1e^{\alpha y} & (y<0)\\ b_2e^{-\beta y} & (y>0).\end{cases} \tag{40}$$

TABLE II. Constants for the surface electron density profile of Eq. (40).

b_0	−0.621	a_{es}	1.625 44
b_1	0.085 758	a_0	1.618 72
b_2	0.464 758	a_2	0.079 101 3
α	2.988 93	a_4	0.028 921 6
β	0.784 656	a_x	0.770 618
$\Phi(0)$	0.754 863	a_{ps}	2.362 14
$\Phi(-\infty)$	1.366 28		

The parameters are displayed in Table II. b_0 is chosen to match the asymptotic ($y \to -\infty$) density in the Thomas-Fermi[28] approximation for jellium (in which $\gamma = 1$), b_2 is chosen to match the Thomas-Fermi jellium value for $n(0)$, and the other three parameters are fixed by Eq. (36) and by continuity of $n(x)$ and dn/dx.

As in Ref. 18, the problem is to minimize

$$\sigma = \frac{k_F^{9/2}}{27\pi^2}\left[\frac{a_{es}}{3\gamma^3} - \frac{a}{\gamma} + \frac{a_2\gamma}{k_F} + \frac{a_4\gamma^3}{3k_F^2}\right], \tag{41}$$

where

$$a = a_0 - \frac{a_x + a_c(\bar{n})}{k_F} + a_{ps}\frac{\langle \delta v \rangle_{WS}}{k_F^2/2}. \tag{42}$$

The constants a_{es}, a_0, a_2, a_4, a_x, and $a_c(\bar{n})$ are defined as functionals of f in Ref. 18, and

$$a_{ps} = \frac{-9}{2}\left[\frac{\pi}{4}\right]^{1/2}\int_{-\infty}^{0} dy[f(y)-1]. \tag{43}$$

Values of these constants for the shape function of Eq. (40) are presented in Table II. The correlation constant $a_c(\bar{n})$ was evaluated numerically and fitted to high accuracy for all r_s by the form

$$a_c(\bar{n}) = \frac{r_s}{14.65 + 5\sqrt{r_s} + 1.425 r_s}. \tag{44}$$

The minimization problem $d\sigma/d\gamma = 0$ reduces to a cubic

TABLE III. Jellium surface properties, calculated within the local-density approximation of Eq. (15) and Ref. 21. KS, Kohn-Sham orbital solution; TFDGW4, exact minimization of Thomas-Fermi-Dirac-Gombas-Weizsäcker-4 functional; This work, one-parameter minimization of the TFDGW4 functional.

r_s (bohr)		σ (erg/cm^2)	W (eV)	x_0 (bohr)
2	KS	−861.5	3.78	1.58
	TFDGW4	−946.5	3.42	1.63
	this work	−899.6	3.66	1.76
4	KS	163.4	2.90	1.23
	TFDGW4	136.4	2.70	1.02
	this work	155.2	2.81	0.90
6	KS	59.4	2.25	1.11
	TFDGW4	48.6	2.14	0.79
	this work	59.8	2.24	0.59

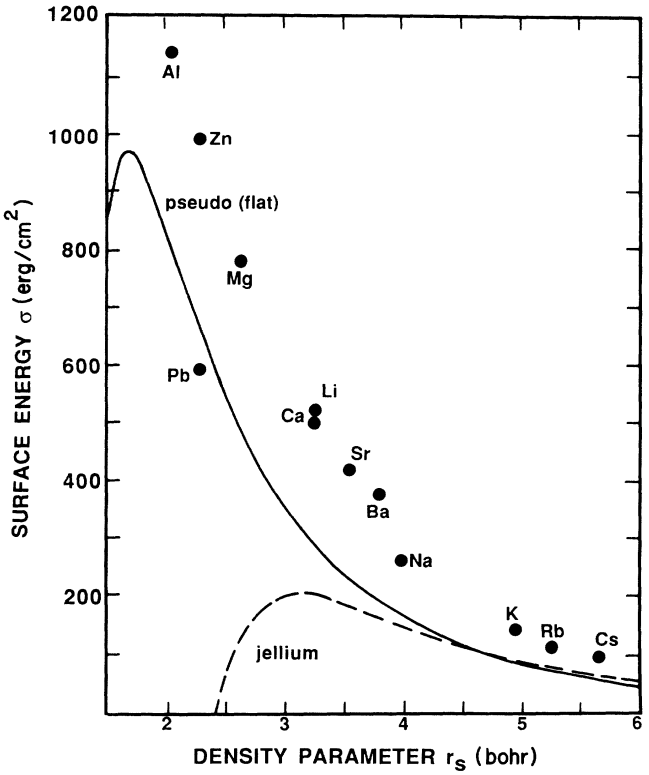

FIG. 2. Surface energy calculated here for jellium and for a flat surface within the structureless pseudopotential model (solid curve), compared with measured liquid-metal surface tensions (dots) extrapolated to zero temperature.

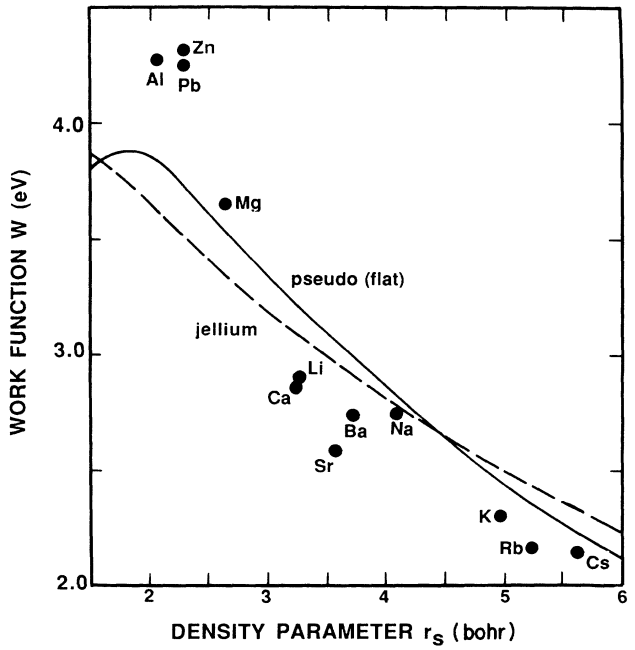

FIG. 3. Work function calculated here for jellium and for a flat surface within the structureless pseudopotential model (solid curve), compared with measured polycrystalline work functions (dots).

equation for γ^2, which is solved analytically; there is only one positive root for each metal.

The work function of Eq. (37) becomes

$$W=\frac{k_F^2}{3\gamma^2}\Phi(0)-\tfrac{3}{10}k_F^2+\frac{3k_F}{4\pi}-\varepsilon_c(\bar{n})+\langle\delta v\rangle_{\rm WS}[f(0)-1], \tag{45}$$

where

$$\Phi(y)=\begin{cases}\dfrac{b_2}{\beta^2}e^{-\beta y} & (y>0)\\ \dfrac{b_2}{\beta^2}-\left[b_0+\dfrac{b_1}{\alpha^2}\right]+b_0e^{y}+\dfrac{b_1}{\alpha^2}e^{\alpha y} & (y<0)\end{cases} \tag{46}$$

is the shape function for the jellium electrostatic potential.

Before presenting our new results, we pause to study the accuracy of our approximations in the case of the jellium surface (Table III). We achieve a one-parameter minimization of the Thomas-Fermi-Dirac-Gombas-Weizsäcker-4 (TFDGW4) energy functional, which has also been minimized exactly via the solution of the Euler equation.[29] Evidently our surface energies lie somewhat above the exact TFDGW4 surface energies. In fact, our variational error tends to cancel the error of the gradient expansion of Eq. (16), and so our results simulate those obtained from the solution of the Kohn-Sham equations,[30] in which the kinetic energy is treated exactly.

Within the structureless pseudopotential model, the surface energy and work function of a flat surface depend *only* upon r_s. Our results are compared to measured liquid-metal surface tensions[31] (extrapolated to zero temperature) and polycrystalline work functions[32] in Figs. 2 and 3. Evidently the structureless pseudopotential corrections go a long way toward improving the jellium results, especially for the high-density metals.

Nevertheless, the predicted surface energies still lie below experiment. Part of the difference can be eliminat-

TABLE IV. Face-dependent surface properties of the monovalent metals. Our calculated results are reported for the jellium model and for the structureless pseudopotential model (applied to a flat surface and three crystal faces).

	case	$\langle\delta v\rangle_{\rm face}$ (eV)	γ	σ (erg/cm^2)	W (eV)	x_0	$x_0+d/2$ (bohr)
H	jell	0.00	1.23	−5203	3.86	1.87	
(fcc)	flat	−5.20	1.62	922	3.84	0.98	
	111	−4.74	1.58	1060	3.80	1.06	2.23
	100	−3.56	1.48	1124	3.73	1.27	2.28
	110	−1.80	1.35	1269	3.75	1.58	2.30
Li	jell	0.00	1.45	203	3.07	1.14	
(bcc)	flat	−0.43	1.54	280	3.18	0.88	
	110	−0.08	1.47	326	3.09	1.09	3.44
	100	0.99	1.26	371	2.92	1.92	3.59
	111	1.70	1.13	433	2.90	2.56	3.53
Na	jell	0.00	1.49	156	2.81	0.90	
(bcc)	flat	−0.06	1.51	163	2.83	0.86	
	110	0.22	1.44	190	2.75	1.07	3.94
	100	1.10	1.22	216	2.58	2.04	4.07
	111	1.69	1.09	252	2.54	2.86	4.02
K	jell	0.00	1.51	97	2.51	0.71	
(bcc)	flat	0.17	1.46	87	2.45	0.84	
	110	0.40	1.40	111	2.37	1.06	4.62
	100	1.11	1.18	115	2.21	2.18	4.70
	111	1.58	1.04	134	2.17	3.21	4.66
Rb	jell	0.00	1.51	85	2.43	0.67	
(bcc)	flat	0.20	1.45	74	2.36	0.83	
	110	0.42	1.39	86	2.28	1.06	4.81
	100	1.09	1.17	98	2.12	2.21	4.87
	111	1.54	1.03	114	2.08	3.31	4.84
Cs	jell	0.00	1.51	71	2.33	0.63	
(bcc)	flat	0.24	1.44	59	2.24	0.83	
	110	0.45	1.37	69	2.17	1.05	5.10
	110	1.07	1.15	79	2.01	2.26	5.12
	111	1.49	1.01	92	1.97	3.44	5.09

ed by recognizing that the surface of a liquid cannot be flat on the atomic scale; the calculated flat-surface energies should be multiplied by a "corrugation factor"[19] of about 1.2, as discussed in Sec. V. The remaining discrepancy might be corrected by band-structure effects. Except in Pb, it can be eliminated by adding to $\langle \delta v \rangle_{\rm WS}$ in Eq. (35) an energy of about -0.3 ± 0.3 eV, as suggested by Eq. (30); this energy seems to be within the range of band-structure effects. However, corrections to the local-density approximation of Eq. (15) could have a comparable effect.[33]

The predicted work functions for the high-density metals are also somewhat too low. This error might be reduced in self-consistent Kohn-Sham orbital calculations, since the high-density work function is sensitive[30] to the achievement of full self-consistency.

Any excess charge in a metal at equilibrium resides at the surface, where it forms a surface charge density Σ (excess charge per unit area). If Σ is infinitesimal, we may expand the electron density

$$n_\Sigma(x)=n_0(x)-\Sigma g(x)\ , \tag{47}$$

where $g(x)=-\partial n_\Sigma/\partial\Sigma$ is the normalized profile of excess charge:

$$\int_{-\infty}^{\infty} dx\ g(x)=1\ . \tag{48}$$

The centroid of excess charge is located at

$$x_0=\int_{-\infty}^{\infty} dx\ xg(x)\ . \tag{49}$$

We can model this situation by shifting and rescaling the trial electron density profile:

$$n_\Sigma(x)=\bar{n}f(\gamma_\Sigma k_s(x+\Sigma/\bar{n}))\ , \tag{50}$$

$$g(x)=-\bar{n}f'(\gamma_0 k_s x)\left[\frac{\gamma_0 k_s}{\bar{n}}+k_s x\frac{d\gamma_\Sigma}{d\Sigma}\bigg|_{\Sigma=0}\right]\ , \tag{51}$$

TABLE V. Face-dependent surface properties of divalent and polyvalent metals.

	case	$\langle \delta v \rangle_{\rm face}$ (eV)	γ	σ (erg/cm^2)	W (eV)	x_0	$x_0+d/2$ (bohr)
Al	jell	0.00	1.31	−642	3.62	1.73	
(fcc)	flat	−2.49	1.60	801	3.83	0.95	
	111	−1.74	1.51	921	3.72	1.17	3.37
	100	0.12	1.30	977	3.62	1.77	3.68
	110	2.92	1.07	1103	3.81	2.58	3.93
Pb	jell	0.00	1.35	−136	3.51	1.62	
(fcc)	flat	−1.80	1.59	659	3.73	0.94	
	111	−0.99	1.48	758	3.59	1.22	3.92
	100	1.04	1.23	804	3.50	2.05	4.38
	110	4.09	0.97	907	3.77	3.09	4.74
Zn	jell	0.00	1.35	−136	3.51	1.62	
(hcp,$c/a=1.861$)	flat	−1.80	1.59	659	3.73	0.94	
	0001	−2.27	1.66	730	3.83	0.79	3.13
Mg	jell	0.00	1.39	141	3.34	1.44	
(hcp,$c/a=1.625$)	flat	−1.11	1.57	481	3.54	0.92	
	0001	−0.64	1.50	554	3.44	1.12	3.58
Ca	jell	0.00	1.45	203	3.08	1.14	
(fcc)	flat	−0.44	1.54	282	3.19	0.88	
	111	−0.08	1.47	325	3.10	1.09	4.14
	100	0.82	1.29	344	2.94	1.78	4.41
	110	2.17	1.06	389	2.92	2.97	4.83
Sr	jell	0.00	1.47	187	2.96	1.03	
(fcc)	flat	−0.25	1.53	222	3.03	0.87	
	111	0.08	1.46	256	2.94	1.09	4.41
	100	0.90	1.27	271	2.79	1.82	4.69
	110	2.14	1.04	306	2.75	3.14	5.17
Ba	jell	0.00	1.48	177	2.91	0.98	
(bcc)	flat	−0.18	1.52	200	2.96	0.87	
	110	0.31	1.41	233	2.83	1.22	4.58
	100	1.81	1.08	265	2.67	2.87	5.24
	111	2.81	0.92	309	2.73	3.93	5.30

$$x_0=\frac{k_F^2}{6\pi\gamma_0^3}\Phi(-\infty)\left.\frac{d\gamma_\Sigma}{d\Sigma}\right|_{\Sigma=0} . \quad (52)$$

To evaluate $d\gamma/d\Sigma$, we observe that, to first order in Σ, the surface energy is[8,9]

$$\sigma(\Sigma)=\sigma(0)+W\Sigma , \quad (53)$$

where W is the work function of Eq. (37). Now γ_Σ minimizes $\sigma(\Sigma)$, so

$$\left.\frac{d\sigma(\Sigma)}{d\gamma}\right|_{\gamma_\Sigma}=0=\left.\left[\frac{d\sigma(0)}{d\gamma}+\Sigma\frac{dW}{d\gamma}\right]\right|_{\gamma_\Sigma}$$
$$=[F(\gamma)+\Sigma G(\gamma)]|_{\gamma_\Sigma} . \quad (54)$$

This equation defines γ as a function of Σ for small Σ. Thus

$$\left.\frac{d\gamma_\Sigma}{d\Sigma}\right|_{\Sigma=0}=\left.\frac{-G(\gamma)}{F'(\gamma)}\right|_{\Sigma=0}$$
$$=\frac{9\pi^2\Phi(0)k_F^{-5/2}}{a+2a_2\gamma^2/k_F+3a_4\gamma^4/k_F^2} . \quad (55)$$

Equations (52) and (55) generalize a result of Schreier and Rebentrost[34] to real-metal surfaces.

Our calculated centroids x_0 for the jellium surface are presented in Table III. The results for real metals will be discussed in the following section.

V. ATOMIC CORRUGATION AND THE FACE DEPENDENCE OF SURFACE PROPERTIES

As discussed in Sec. II, the positive background $n_+(\mathbf{r})$ in the simplified energy functional (23) should be constant inside and zero outside a sharp surface cut along the exposed boundaries of Wigner-Seitz cells. Each choice of exposed crystal face will have its own degree of atomic corrugation. In principle, then, one must solve a three-dimensional problem[6] to find the electron density and surface energy for each exposed crystal face. Here, we evade this numerically difficult problem by a simulation that requires only one-dimensional calculations like those of Sec. IV.

Atomic corrugation enhances the exposed microscopic surface area (over that for a flat surface) by a "corrugation factor" greater than 1. This factor has been estimated[19] within the Wigner-Seitz-sphere approximation. As discussed in Ref. 19, it is not unreasonable to assume that the surface energy of a corrugated crystal face is enhanced by the same corrugation factor:

$$\sigma_{\text{face}}\approx\frac{2}{1+d/2r_0}\sigma_{\text{flat}} , \quad (56)$$

where σ_{flat} is the flat-surface energy of Sec. IV and d is the distance between neighboring lattice planes parallel to the surface. Table IV of Ref. 7 displays d/r_0 for common crystal faces. The corrugation factor of Eq. (56) varies from 1.15 for the closed-packed fcc (111) face to 1.55 for the "open" bcc (111) face; a reasonable value for a liquid surface in the zero-temperature limit is probably[19] 1.2. Our results for crystals, using Eq. (56), are presented in Tables IV and V.

Atomic corrugation also creates an electrostatic dipole barrier at the surface. As a result, the average value of $\delta v(\mathbf{r})$ over the volume of a semi-infinite crystal depends upon the exposed crystal face, essentially as it does for a lattice of point ions:[7]

$$\langle\delta v\rangle_{\text{face}}=\langle\delta v\rangle_{\text{WS}}+\frac{z}{8r_0}\left[\frac{12}{5}-\left[\frac{d}{r_0}\right]^2\right] . \quad (57)$$

The additional dipole barrier strongly affects the planar average $n(x)$ of the electron density profile, as discovered in Ref. 7.

Following the experience of Monnier and Perdew,[7] we simulate the effect of atomic corrugation upon the electron density $n(x)$, work function W, and centroid of excess charge x_0 by repeating the flat-surface calculations of Sec. IV, with $\langle\delta v\rangle_{\text{WS}}$ of Eqs. (42) and (45) replaced by $\langle\delta v\rangle_{\text{face}}$ of Eq. (57). In Kohn-Sham calculations, this substitution would also be made in Eq. (24).

Our results are presented in Tables IV and V. The displayed scale parameter γ for the electron density profile is strongly face dependent. As discussed in Ref. 7, the electron density effectively screens out the additional dipole barrier in Eq. (57): Although the displayed $\langle\delta v\rangle_{\text{face}}$ depends strongly upon the exposed crystal face, the work function W shows only a weak face dependence.

The distance x_0 from the centroid of excess charge to the jellium edge (Gibbs surface) also depends strongly upon the crystal face, but its distance $x_0+d/2$ from the first lattice plane does not, especially for the monovalent metals. This conclusion conforms with that of Serena, Soler, and Garcia,[35] who studied Al, Pb, and Li using the method of Ref. 7. It suggests a residual "ionic" character of the excess charge at a metal surface.

VI. CONCLUSION

The equilibrium valence electron density (i.e., r_s) is the main parameter that sets the properties of a simple metal. Given r_s alone, the structureless pseudopotential model generates simple, realistic estimates for the cohesive and surface properties, while the jellium model is realistic only for $r_s\approx4$. Properties of the underlying atom, such as its first ionization energy and electron affinity, are also set largely by r_s.[36]

ACKNOWLEDGMENTS

One of us (J.P.P.) acknowledges discussions with J. H. Rose and H. B. Shore. This work was supported in part by the National Science Foundation under Grant No. DMR-88-17866.

[1]N. D. Lang and W. Kohn, Phys. Rev. B **1**, 4555 (1970).
[2]N. D. Lang and W. Kohn, Phys. Rev. B **3**, 1215 (1971).
[3]M. Manninen, Phys. Rev. B **34**, 6886 (1986).
[4]N. W. Ashcroft and D. C. Langreth, Phys. Rev. **155**, 682 (1967).
[5]N. W. Ashcroft, Phys. Lett. **23**, 48 (1966).
[6]J. H. Rose and J. F. Dobson, Solid State Commun. **37**, 91 (1981).
[7]R. Monnier and J. P. Perdew, Phys. Rev. B **17**, 2595 (1978); **22**, 1124(E) (1980).
[8]R. Monnier, J. P. Perdew, D. C. Langreth, and J. W. Wilkins, Phys. Rev. B **18**, 656 (1978).
[9]V. Sahni, J. P. Perdew, and J. Gruenebaum, Phys. Rev. B **23**, 6512 (1981).
[10]K. -P. Bohnen and S. C. Ying, Solid State Commun. **30**, 301 (1979).
[11]C. A. Utreras-Díaz and H. B. Shore, Phys. Rev. B **40**, 10 345 (1989).
[12]J. Hammerberg and N. W. Ashcroft, Phys. Rev. B **9**, 409 (1974).
[13]H. K. Mao and R. J. Hemley, Science **244**, 1462 (1989).
[14]C. A. Utreras-Díaz and H. B. Shore, Phys. Rev. Lett. **52**, 2335 (1984).
[15]J. H. Rose and H. B. Shore, Bull. Am. Phys. Soc. **35**, Abs. **G18**, 8 (1990).
[16]J. P. Perdew, H. Q. Tran, and E. D. Smith, Bull. Am. Phys. Soc. **35**, Abs. G18, 4 (1990).
[17]J. W. Allen and S. A. Rice, J. Chem. Phys. **67**, 5105 (1977).
[18]J. P. Perdew, Phys. Rev. B **21**, 869 (1980).
[19]J. P. Perdew, Y. Wang, and E. Engel (unpublished).
[20]W. Kohn and L. J. Sham, Phys. Rev. **140**, A1133 (1965).
[21]S. H. Vosko, L. Wilk, and M. Nusair, Can. J. Phys. **58**, 1200 (1980).
[22]J. P. Perdew and A. Zunger, Phys. Rev. B **23**, 5048 (1981).
[23]C. H. Hodges, Can. J. Phys. **51**, 1428 (1973).
[24]J. P. Perdew, Phys. Rev. B **25**, 6291 (1982).
[25]C. E. Moore, *Ionization Potentials and Ionization Limits Derived from the Analysis of Optical Spectra,* Nat. Stand. Ref. Data. Ser. No. 34 (National Bureau of Standards, Washington, D.C., 1970).
[26]C. Kittel, *Introduction to Solid State Physics,* 6th ed. (Wiley, New York, 1986).
[27]J. P. Perdew and V. Sahni, Solid State Commun. **30**, 87 (1979).
[28]N. D. Lang, in *Solid State Physics,* edited by H. Ehrenreich, F. Seitz, and D. Turnbull (Academic, New York, 1973), Vol. 28, p. 225.
[29]E. Engel and J. P. Perdew, Phys. Rev. B (to be published).
[30]J. P. Perdew and Y. Wang, Phys. Rev. **B 38**, 12 228 (1988).
[31]W. R. Tyson and W. A. Miller, Surf. Sci. **62**, 267 (1977).
[32]H. B. Michaelson, J. Appl. Phys. **48**, 4729 (1977).
[33]Z. Y. Zhang, D. C. Langreth, and J. P. Perdew, Phys. Rev. B **41**, 5674 (1990).
[34]F. Schreier and F. Rebentrost, J. Phys. C **20**, 2609 (1987).
[35]P. A. Serena, J. M. Soler, and N. Garcia, Europhys. Lett. **8**, 185 (1989).
[36]J. P. Perdew, Phys. Rev. B **37**, 6175 (1988).